

# Semi-Real Evaluation, and Adaptive Control of a 6DOF Surgical Robot

Farzam Tajdari  
School of Engineering  
Delft University of Technology  
Delft, Netherlands  
[f.tajdari@tudelft.nl](mailto:f.tajdari@tudelft.nl)

Naeim Ebrahimi Toulkani  
Aerospace Engineering  
Sharif University of Technology  
Tehran, Iran  
[naeim.ebrahimi@alum.sharif.edu](mailto:naeim.ebrahimi@alum.sharif.edu)

Nima Zhilakzadeh  
Mechanical Engineering  
I.K.I University  
Qazvin, Iran  
[Nimazhilak@gmail.com](mailto:Nimazhilak@gmail.com)

**Abstract**— Surgical robotic revolution has not just assisted surgeons to perform sophisticated surgeries, but also increased accuracy, reduced risk, operative and recovery time. Parallel mechanisms are widely used for designing of surgical robots due to their advantage of low inertia and high precision. Specific surgical procedures confine and restrict their workspace, while controlling and validating the robots are complicated based on their complex dynamic. To this end, in this paper, a 6-DOF robot, with linear manipulators, is designed and controlled. Addressing the inherent nonlinearity of the system, an adaptive PID controller is employed and validated with nonlinear model. The main objective of the paper is implementing the controller using MATLAB on the nonlinear model designed in Adams software as online. Furthermore, as feasibility study, a 3-axis gyro sensor is calibrated and used to produce complex real movements and desires, which is sending real time signals to MATLAB with microcontroller ATmega 2560. Simulation result shows that the adaptive controller identifies the system's dynamic and proceed in error reduction path. In addition, the method defines the workspace of both the states and forces which can be an introduction to comprehensive design of such robots.

**Keywords**— parallel robot, validation, adaptive control, nonlinear parameter

## I. INTRODUCTION

By utilizing the surgical robots, enormous achievements are accomplished such as more accurate surgeries, shorter surgery time and recovery time of patients. From kinematic structure point of view, surgical robots are sorted in three categories named serial, parallel and hybrid architecture [1]. Regarding to wide usage range of Serial robots, it is most common in medical field except the applications which need more accuracy because Serial robots are not reliable in this field. To overcome this issue, the design turns into parallel which is more precious [2]. The first robot that was used for human brain biopsy was PUMA 560 in 1985 and after that a robot named ROBODOC™ 5 axis SCARA robot including 2 revolute joint axes was used in 1998 which was accepted by Food and Drug Administration (FDA) for total hip replacement [3],[4]. In [5], the advanced surgical serial design is illustrated with notice to required workspace with constrained outlined. Another robot which succeeded to be certified by FDA in 2000 for general laparoscopic surgeries [6] is Da Vinci that has a reputation for most popular serial robot. A thriving Israeli team of researchers introduced the Miniature Robot for Surgical (MARS) procedures [7] with six degree of freedom (DOF) parallel manipulator, 10 cm<sup>3</sup> work volume and 557 cm<sup>3</sup> size in 2003. One of the most remarkable features of MARS is its light weight (200g) that makes registration process much easier. The robot has application to pedicle screw in spinal fusion and distal locking in intramedullary nailing [8], [9]. MARS improved

to Spine Assist and then to Renaissance that are released by Mazor Robotics (Cesarea, Israel). Kobler et al. invented a parallel kinematic robot based on Stewart-Gough platform for skull surgery that could be mounted on head. It benefits from spherical heads which are installed on patient skull [10]. The moving platform helps robot for better intervention between the bone anchors e.g. drilling access to cochlea, insertion of needle etc. [10], which specifies the need of control for the robot. Many tasks performed by robot manipulators require the interaction between the end effector and its environment, such as pushing, scraping, deburring, grinding, pounding, polishing, twisting, cutting, excavating. In some of the mentioned applications, robot position control is necessary and in some others, force control is desired. There are several methods to force control of robots, including stiffness control, impedance control, admittance control, hybrid control, explicit force control and implicit force control [11], [12], [13], [14]. Thus, this paper aims to not only design a controller for the complicated mechanism, but also, validate the controller on a nonlinear system through Adams software which less has been studied recently. Paper is organized as follow: Dynamic equation of Stewart robot is presented in II while controller design is laid in section III. Simulation Setup, results, and conclusion are presented in section IV, V and VI respectively.

## II. DYNAMIC EQUATION OF STEWART PLATFORM

In this section, dynamic equations of Stewart mechanism are derived using Newton-Euler method. The derivations are summarized just to show different dynamic features of the systems, and the affects. Stewart mechanism studied in this paper, is depicted in Fig. 1, which consists of an endeffector, a fixed platform as base, and six legs as manipulators to move the end effector. The legs are connected both from end effector to base platform by spherical joints.

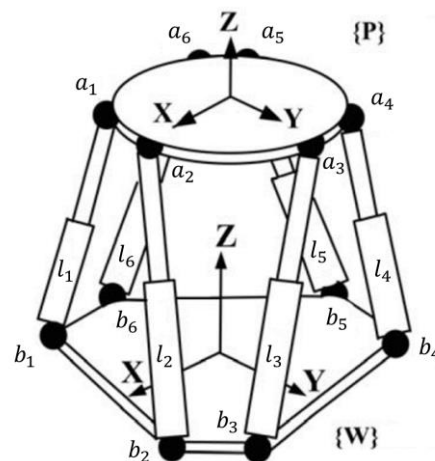


Fig. 1. Stewart platform mechanism.

### A. Legs' dynamic analysis

Considering legs complete rotation equilibrium (consisting up and down sections) according to Fig. 2, the equilibrium momentum equation can be written around the joints as below.

$$\begin{aligned} r_u \times m_u G + r_d \times m_d G + l_i n_i \times F_i^n + C_u w_i + C_s (w_i - \omega_p) \\ = r_u \times m_u \ddot{a}_{ui} + r_d \times m_d \ddot{a}_{di} + (I_u + I_d) \alpha_i + w_i \times \\ (I_u + I_d) w_i \end{aligned} \quad (1)$$

At above equation,  $r_d$  and  $r_u$  are Center of Gravity (CG) vectors,  $I_d$  and  $I_u$  are mass moments of inertia,  $m_d$  and  $m_u$  are masses. And  $\ddot{a}_{di}$  and  $\ddot{a}_{ui}$  are acceleration of up and down sections,  $G$  is acceleration of gravity,  $F_i^n$  is applied force from platform to legs (in the general coordinates of fixed platform),  $\alpha_i$  and  $w_i$  are acceleration and rotational velocity of legs vectors,  $w_i$  is rotational velocity vector of platform  $C_s$  and  $C_u$  are viscous friction coefficients in spherical and universal joints. Anyway, the  $F_i^n$  is not the force that may cause-motion for calculation of motion-cause force, the upper section of leg shall study and the forces acting at the leg shall considered:

$$m_u n_i G + F_i + n_i F_i^n - C_p i_i = m_u n_i \ddot{a}_{ui} \quad (2)$$

In the above equation  $F_i$  is the acting force from (driver, motive/ stimulus) and  $C_p i_i$  is the result of amortization (viscous friction) in the slider joint,  $n_i$  is unit vector of legs and  $C_p$  is the viscous friction coefficient.

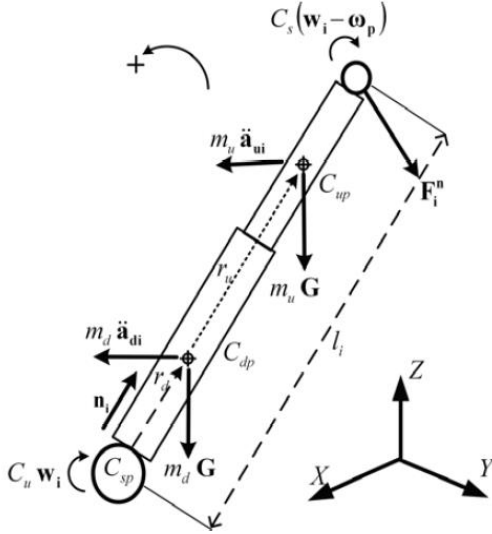


Fig. 2. Free body diagram of forces applied to hezapas's leg.

### B. Platforms' dynamic equation: (Newton-Euler equilibrium)

According to free diagram shown in Fig. 3 and Newton-Euler equation, dynamic equation of the robot is described as below equation.

$$M_p G + {}^W R_p F_{ext} - \sum_{i=1}^6 F_i^n = M_p \ddot{x}_g \quad (3)$$

In this equation  $M_p$  is the platform's mass,  $\ddot{x}_g$  is the CG acceleration of end effector and  $F_{ext}$  is the external acting force on platform and  ${}^W R_p$  is the rotation matrix of final motive enforcer.

$${}^W R_p = \begin{bmatrix} C\theta_z C\theta_y & -S\theta_z C\theta_z + C\theta_z S\theta_y S\theta_x & S\theta_z S\theta_x + C\theta_z S\theta_y C\theta_x \\ S\theta_z C\theta_y & C\theta_z C\theta_z + S\theta_y S\theta_z S\theta_x & -C\theta_z S\theta_x + S\theta_z S\theta_y C\theta_x \\ -S\theta_y & C\theta_y S\theta_x & C\theta_y C\theta_x \end{bmatrix} \quad (4)$$

where, we assumed  $C\theta_x = \text{Cos}(\theta_x)$ ,  $S\theta_x = \text{Sin}(\theta_x)$ . Also momentum equilibrium (Euler) is considered toward central point of platform:

$$M_p \bar{r} \times G + {}^W R_p (M_{ext} + GC \times F_{ext}) + \sum_{i=1}^6 ({}^W R_p {}^P a_i \times F_i^n) + \sum (C_u w_i + C_s (w_i - \omega_p)) = M_p \bar{r} \times \ddot{x}_g + I_p \alpha_p + \omega_p \times I_p \omega_p \quad (5)$$

In (5),  $F_{ext}$  is the external momentum, CG is the position vector of reacting force on end effector,  $\bar{r}$  is the position vector of end effector's CG,  $I_p$  is the moment of inertia of the end effector in the reference coordinates  $\{W\}$  and  ${}^P a_i$  is the spherical joint points vector in the end effector's motive coordinates. In Fig. 3 the center gravity and center of geometry are coincident.

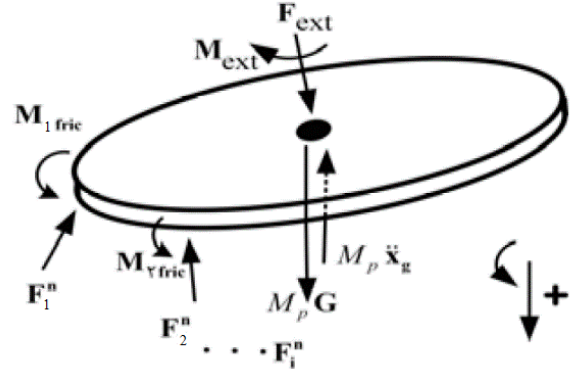


Fig. 3. Free body diagram of forces applied to endeffector.

### C. Complete dynamic equation of Stewart mechanism

By combining of two force equations (1), and (2) and two momentum equations (4), and (5) of moving platform, the dynamic system of equations of six legs is derived as below:

$$M \begin{bmatrix} \ddot{x}_g \\ \alpha_p \end{bmatrix} + \eta = J^{-1} F + \begin{bmatrix} {}^W R_p F_{ext} \\ {}^W R_p (M_{ext} + GC \times F_{ext}) \end{bmatrix} \quad (6)$$

$J^{-1}$  is inverse Jacobean matrix in (7),  $M$  is inertial matrix and  $\eta$  is consisting moments and gravitation Coriolis forces.

$$J^{-1} = \begin{bmatrix} n_1^T & ({}^W R_p P_{a_1} \times n_1)^T \\ \vdots & \vdots \\ n_6^T & ({}^W R_p P_{a_6} \times n_6)^T \end{bmatrix} \quad (7)$$

As it can be considered solving the equations system of (6) all kinematic variables (position, velocity, acceleration and physical characteristic of structure) and dynamic parameters (mass, moments of inertia of each component, forces and external moments) of end effector shall put in wrote software. Then solving the system of (6) and finding the acting forces on each leg is easily applicable by Newton-Raphson method.

### D. ADAMS simulation of Stewart dynamic

As the aim of calculating the system dynamic is to build a high accuracy robot surgery, having a simulation environment (ambient) that owns the ability of considering of all nonlinear parameters will be useful.

As some constraints could not be considered in MATLAB software (such as: collision, hardness and elasticity of bodies, friction and the volume of bodies), the ADAMS software will be utilized in this paper in order to simulation of hexapod robot's dynamic model. The only problem with ADAMS software is that the nonlinear controlled could not be implemented directly, thus in order to control the nonlinear system, the software is connected to MATLAB and controlled online.

Firstly, the system is designed in SOLIDWORKS (see Fig. 4), then the mentioned design is imported to ADAMS and the essential constraint such as joints' constraint, mass and materials of members the bodies rigidity toward each other and friction are applied on it. The information about design assumption are presented in Table I. As it is shown in Table I, the system has 14 component of mass, the number and moment of inertias.

As it is specified in Fig. 5(a) and (b), the constraints are applied on the system. Also, it is assumed a bidirectional force on each leg that is shown with red colour.

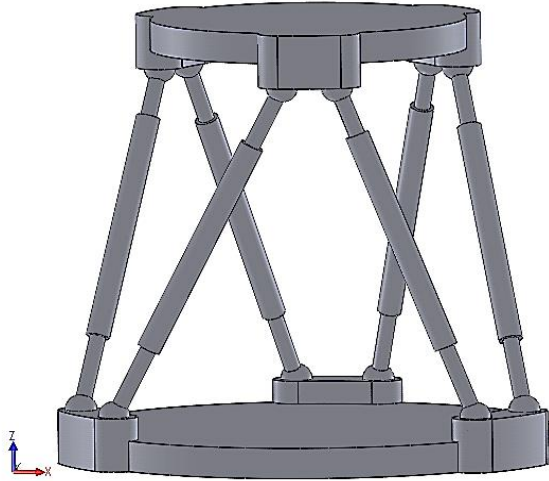
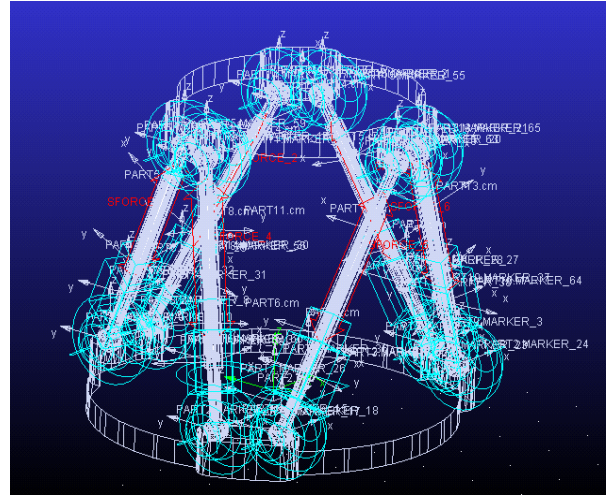


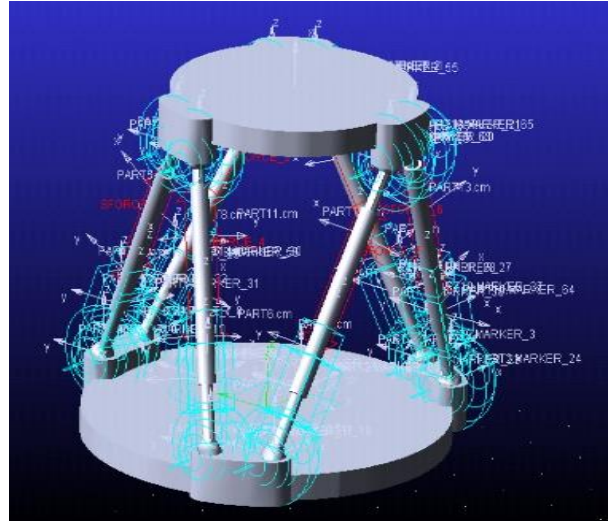
Fig. 4. Designed system in solidworks software.

TABLE I. DYNAMIC SYSTEM PARAMETERS.

Qty.	Dimension(cm)	Inertia (kg.m <sup>2</sup> )	Mass (kg)	Parts
6	25	$I_x=0.002$	0.75	Upper parts of links
		$I_y=0.002$		
		$I_z=0.0001$		
6	25	$I_x=0.003$	1	Lower parts of links
		$I_y=0.003$		
		$I_z=0.00012$		
1	Circle(R=10)	$I_x=0.012$	3	End effector
		$I_y=0.062$		
		$I_z=0.062$		
1	Circle(R=15)	$I_x=0.054$	6.5	Base
		$I_y=0.027$		
		$I_z=0.027$		



(a)



(b)

Fig. 5. Designed system with constraints in ADAMS Software. (a) Lucid view. (b) Opaque view.

### III. CONTROLLING HEXAPOD'S DYNAMICS

As mentioned, the designed dynamic system in the ADAMS software is very nonlinear. Thus in order to control the system a robust controller shall be utilized, that should be able to identify nonlinear parameters online.

#### A. Adaptive controller designing:

Assuming that, the dynamic equation of system is written as  $\dot{x} = f(x, \dot{x}) + bu$ , the controller would be considered as below:

$$u = P_{2n \times 2n} E_{2n \times 1} \quad (8)$$

Where  $P$  is controller parameters, and  $E$  is error of controllable states with desires. Considering the input of the controller as (8) always satisfies converging adaptive controller parameters, according to 1-8 Lema in [12]. Moreover, if parameters in each steps of stimulated run, changes with below rate, the system is stable.

$$\dot{P} = -\gamma_{2n \times 2n} \times E \times V^T \quad (9)$$

In (9), state variables vector is  $V = [x_{n \times 1}; \dot{x}_{n \times 1}]$ ,  $E = V - V_d$  is the error of state variables vector, and  $\gamma$  is converging rate of parameters. While, the stimulation of



parameters is done by (9) this action will be continued until cancellation of the error. In order to evaluation of controller performance, the existing dynamic is controlled online in ADAMS software using MATLAB. The controlling diagram the whole system is showed in Fig. 6.

### B. Stability analysis

The system dynamic can be considered as follows:

$$M\ddot{\theta} = -c_p f(\theta) + b_p u \quad (10)$$

where matrix  $M$ ,  $c_p$  and  $b_p$  are system's coefficients.

Considering  $\dot{\theta}_1 = \dot{\theta} = \dot{\theta}_2$  and  $\dot{\theta}_2 = \dot{\theta} = \frac{1}{M}(-c_p f(\theta) + b_p u)$  system' states can be written as:

$$\dot{\theta} = \begin{bmatrix} 0 & 1 \\ 0 & 0 \end{bmatrix} \theta + \frac{-c_p}{M} \begin{bmatrix} 0 \\ f(\theta) \end{bmatrix} + \frac{b_p}{M} \begin{bmatrix} 0 \\ u \end{bmatrix} \quad (11)$$

where,

$$\dot{\theta} = \begin{bmatrix} 0_{2 \times 2} & I_{2 \times 2} \\ 0_{2 \times 2} & 0_{2 \times 2} \end{bmatrix} \theta + \begin{bmatrix} 0_{2 \times 1} \\ M^{-1}(-c_p) \end{bmatrix} f(\theta) + \begin{bmatrix} 0_{2 \times 1} \\ M^{-1}(b_p) \end{bmatrix} u \quad (12)$$

By considering  $a_p = -\begin{bmatrix} 0 & 1 \\ 0 & 0 \end{bmatrix}$ ,  $c_p = \begin{bmatrix} 0 & -c_p \\ 0 & M \end{bmatrix}$ ,  $f(\theta) = \begin{bmatrix} 0 \\ f(\theta) \end{bmatrix}$  and  $b_p = \begin{bmatrix} 0 & 0 \\ 0 & b_p \\ 0 & M \end{bmatrix}$ ,  $u = \begin{bmatrix} 0 \\ u \end{bmatrix}$ , system dynamic can be shown as:

$$\dot{\theta} = -a_p \theta + c_p f(\theta) + b_p u \quad (13)$$

We suppose that  $u$ , the control efforts, is equal to:

$$u = \hat{a}_\theta \theta + \hat{a}_f f(\theta) + \hat{a}_r r \quad (14)$$

where variable  $r$  represents the desired values of states( $\theta$ ).

For designing a PID controller, we know that this control effort should be considered as:

$$u = [P, I, D]e \quad (15)$$

where,  $P = \begin{bmatrix} P, I \int dt, D \frac{d}{dt} \end{bmatrix}$ ,  $e = \theta - r$ ,  $u_{PID} = PE$ . Supposing  $P = [P, I, D]$ , and  $e = [\theta - r]$ , then,

$$u = P\theta - Pr \quad (16)$$

Thus, by comparing the last two equations we have:

$$u = u_{PID} + u_{nonlinear} \quad (17)$$

Assuming  $\hat{a}_\theta = P$  and  $\hat{a}_r = -P$  then (17) changes to:

$$u = \hat{a}_\theta \theta + \hat{a}_r r + \hat{a}_f f(\theta) \quad (18)$$

Consequently,

$$\dot{\theta} = -a_p \theta + c_p f(\theta) + b_p u = -a_p \theta + c_p f(\theta) + b_p \hat{a}_\theta \theta + b_p \hat{a}_r r + b_p \hat{a}_f f(\theta) \quad (19)$$

The reference model has been considered as:

$$\dot{\theta}_M = -a_M \theta_M + b_M r \quad (20)$$

The dynamic of error can be obtained from:

$$\dot{e} = \dot{\theta} - \dot{\theta}_M = -a_M(\theta - \theta_M) + (a_M - a_p + b_p \hat{a}_\theta)\theta + (b_p \hat{a}_r - b_m)r + c_p f(\theta) + b_p \hat{a}_f f(\theta) \quad (21)$$

After simplification:

$$\dot{e} = -a_M e + b_p(\hat{a}_r r + \hat{a}_\theta \theta) - c_p f(\theta) + b_p \hat{a}_f f(\theta) \quad (22)$$

And:

$$\dot{e} + a_M e = b_p \left\{ \hat{a}_r r + \hat{a}_\theta \theta + \underbrace{\left( \hat{a}_f - \frac{c_p}{b_p} \right)}_{\hat{a}_f} f(\theta) \right\} \quad (23)$$

Considering,  $\dot{e} = Se$ ,

$$e = \frac{b_p}{s+a_M} [\tilde{a}_r \tilde{a}_\theta \tilde{a}_f] \begin{bmatrix} r \\ \theta \\ f(\theta) \end{bmatrix} \quad (24)$$

According to (24), dynamic of error is stable as  $a_M$  is a positive number, if the values of  $\tilde{a}_r$ ,  $\tilde{a}_\theta$  and  $\tilde{a}_f$  are converging. For proving that the parameters are convergence and using Lyapunov function, we suppose:

$$\begin{cases} \dot{V} = \theta^T P \theta + \tilde{a}^T \Gamma^{-1} \tilde{a} \\ \dot{\theta} = A\theta + bu \\ e = c\theta, c = \mathbb{P}b \\ u = V^T \tilde{a} \\ \mathbb{P}A + A^T \mathbb{P} = -Q (Q = Q^T > 0), \\ \dot{V} = -\theta^T Q \theta + 2\tilde{a}^T V b^T P \theta + 2\tilde{a}^T \Gamma^{-1} \dot{\tilde{a}}. \end{cases} \quad (25)$$

Due to making sure that the value of  $\dot{V}$  is minus, it is just enough that the value of following terms becomes zero:

$$2\tilde{a}^T V b^T P \theta + 2\tilde{a}^T \Gamma^{-1} \dot{\tilde{a}} = 0 \rightarrow \dot{\tilde{a}} = -\Gamma V b^T P \theta \quad (26)$$

Considering,  $e = c\theta$ , and  $c = \mathbb{P}b$ , the adaptive rule is,

$$\dot{\tilde{a}} = -\Gamma e^T V. \quad (27)$$

### IV. DESIRED POSITION IMPLEMENTATION BY A GYRO SENSOR

As validation of the controller, desired position will import to the MATLAB by serial port and using a gyro sensor and Arduino at mega 2560 board. This sensor is an ADXL335 type sensor and it is only able to measure the acceleration in 3 axes of the reference connected to it. In order to get the Eulerian angles by the acceleration of ADXL335 sensor, according to (4) every point in the coordinate system that is connected to earth can be transited to coordinate system connected to end effector and assuming the gravity direction is through Z (in earth-connected coordinate system) the rotational angles in X and Y axes can be derived as.

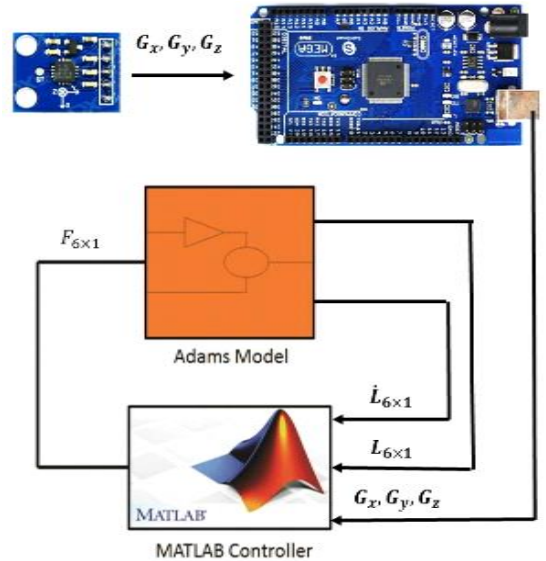


Fig. 6. Connectivity diagram of used sensor and softwares.

$${}^w R_P \begin{bmatrix} G_x \\ G_y \\ G_z \end{bmatrix} = \begin{bmatrix} 0 \\ 0 \\ 1 \end{bmatrix} \quad (28)$$

$$\begin{bmatrix} G_x \\ G_y \\ G_z \end{bmatrix} = {}^w R_P^{-1} \begin{bmatrix} 0 \\ 0 \\ g \end{bmatrix} \quad (29)$$

As the  ${}^w R_P$  is a translation vector, thus  ${}^w R_P^{-1} = {}^w R_P$ , and determinant of the matrix is one. Accordingly, the equations will simplify to.

$$\frac{G_P}{\|G_P\|} = \frac{1}{\|G_P\|} \begin{bmatrix} G_x \\ G_y \\ G_z \end{bmatrix} = \begin{bmatrix} -S\theta \\ C\theta S\phi \\ C\theta C\phi \end{bmatrix} g \quad (30)$$

So the Eulerian angles will be derived as follow:

$$\tan\phi_{xyz} = \left( \frac{G_{py}}{G_{pz}} \right) \quad (31)$$

$$\tan\theta_{xyz} = \left( \frac{-G_x}{G_y S\phi + G_z C\phi} \right) = \frac{-G_x}{\sqrt{G_y^2 + G_z^2}} \quad (32)$$

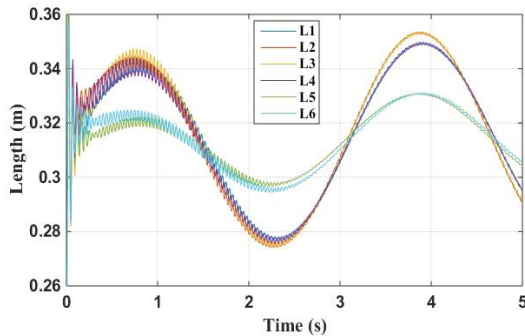
## V. EXPERIMENT RESULTS

Previously explained, the simulation control desired angles receiving and sending process are shown in Fig. 6 simultaneously. Also, controller's performance and the way of parameters estimation are shown in Fig. 7. In this figure, the desired amounts are inputted as below and the other amount are assumed as zero. The angles amounts are produced by accelerometer sensor.

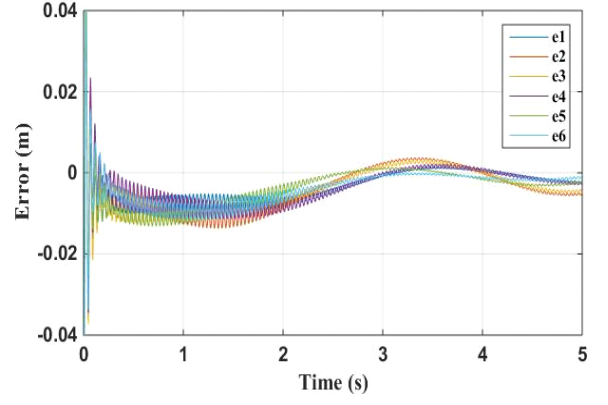
$$\phi(t) = \frac{\pi}{6} \sin(2t) \quad (33)$$

$$Z = 0.05 \sin(2t) + 0.3 \quad (34)$$

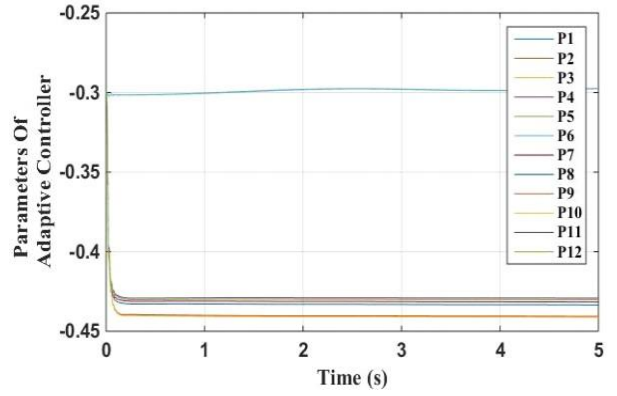
Furthermore,  $\gamma_{2n \times 2n}$  is considered as  $0.1I_{2n \times 2n}$  as controller parameter and the initial condition of all other controller ratios are -0.3. Considering Fig. 7(c), identification and estimation are done as well, and the parameters of controller are converged. Actually, the adaptive controller has identified the system in less than 1 second, thus the errors are reduced after this converging and the system is going to trace the target (sensor's data) with the minimum error. Furthermore, force trajectories on system are shown in Fig. 7(d) that are valuable to choose electromotor and system designing for manufacturing, considering ADAMS as a powerful tool to simulate real environment. Furthermore, it can be observed from Fig. 7(c), the tracing error is decreased after passing the time and identifying the system's dynamic by control more accurate. Which is one of the advantages of adaptive controllers.



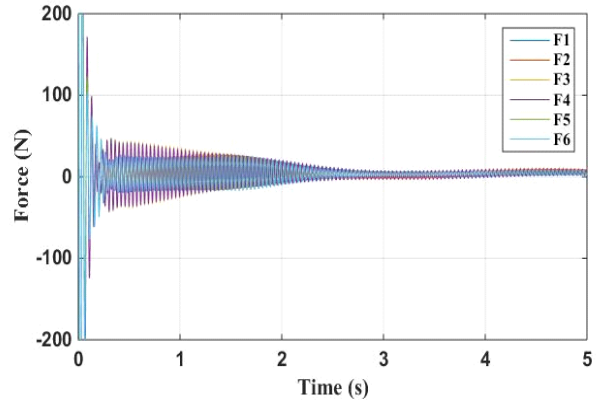
(a)



(b)



(c)



(d)

Fig. 7. Adaptive controller performance. (a) Length of links. (b) Tracing error. (c) Controller parameters. (d) Applied forces from controller to each link.

## VI. CONCLUSION

Parallel robots are suitable for some surgery operations as they are more accurate and faster, with lower inertia and higher precision compression to other robotic mechanisms. Accordingly, in this paper, a parallel robot was introduced as surgical robot, controlled by implementing adaptive PD controller and validated with a non-linear model in ADAMS online. Also, one of the other goals of this paper is to study the fabrication feasibility of the robot. Finally, the simulation results showed that the adaptive controller was able to identify dynamic of system and proceeded in the way of minimizing error and complete tracking. After ample experiments, and improving the robot dynamics, manufacturing the robot,

sensitivity analysis of controller parameters are the topics that will be appeared in our future publications.

#### REFERENCES

- [1] N. Simaan, "Analysis and synthesis of parallel robots for medical applications," Ph.D. dissertation, Technion-Israel Institute of Technology, Faculty of Mechanical Engineering, 1999.
- [2] Z. Pandilov and V. Dukovski, "Comparison of the characteristics between serial and parallel robots," *Acta Technica Corviniensis-Bulletin of Engineering*, vol. 7, no. 1, p. 143, 2014.
- [3] P. Kazanzides, J. Zuhars, B. Mittelstadt, B. Williamson, P. Cain, F. Smith, L. Rose, and B. Musits, "Architecture of a surgical robot," in *Systems, Man and Cybernetics, 1992.*, IEEE International Conference on. IEEE, 1992, pp. 1624–1629.
- [4] A. P. Schulz, K. Seide, C. Queitsch, A. Von Haugwitz, J. Meiners, B. Kienast, M. Tarabolsi, M. Kammal, and C. Jürgens, "Results of total hip replacement using the robodoc surgical assistant system: clinical outcome and evaluation of complications for 97 procedures," *The International Journal of Medical Robotics and Computer Assisted Surgery*, vol. 3, no. 4, pp. 301–306, 2007.
- [5] M. A. Laribi, M. Arsicault, T. Riviere, and S. Zeghloul, "Toward new minimally invasive surgical robotic system," in *Industrial Technology (ICIT), 2012 IEEE International Conference on.* IEEE, 2012, pp. 504–509.
- [6] C.-H. Kuo and J. S. Dai, "Robotics for minimally invasive surgery: a historical review from the perspective of kinematics," in *International symposium on history of machines and mechanisms.* Springer, 2009, pp. 337–354.
- [7] M. Shoham, M. Burman, E. Zehavi, L. Joskowicz, E. Batkilin, and Y. Kunicher, "Bone-mounted miniature robot for surgical procedures: Concept and clinical applications," *IEEE Transactions on Robotics and Automation*, vol. 19, no. 5, pp. 893–901, 2003.
- [8] Z. Yaniv and L. Joskowicz, "Precise robot-assisted guide positioning for distal locking of intramedullary nails," *IEEE transactions on medical imaging*, vol. 24, no. 5, pp. 624–635, 2005.
- [9] Z. Yaniv and L. Joskowicz, "Robot-assisted distal locking of long bone intramedullary nails: Localization, registration, and in vitro experiments," in *International Conference on Medical Image Computing and Computer-Assisted Intervention.* Springer, 2004, pp. 58–65.
- [10] J.-P. Kobler, J. Kotlarski, J. Oltjen, S. Baron, and T. Ortmaier, "Design and analysis of a head-mounted parallel kinematic device for skull surgery," *International journal of computer assisted radiology and surgery*, vol. 7, no. 1, pp. 137–149, 2012.
- [11] E. Akdoğan, M. E. Aktan, A. T. Koru, M. S. Arslan, M. Atlıhan, & B. Kuran. "Hybrid impedance control of a robot manipulator for wrist and forearm rehabilitation: Performance analysis and clinical results". *Mechatronics*, 49, 77-91, 2018.
- [12] H. Navvabi, & A. H. Markazi. "Hybrid position/force control of Stewart Manipulator using Extended Adaptive Fuzzy Sliding Mode Controller (E-AFSMC)". *ISA transactions*, 88, 280-295, 2019.
- [13] H. Navvabi, & A. H. D. Markazi. "New AFSMC method for nonlinear system with state-dependent uncertainty: Application to hexapod robot position control". *Journal of Intelligent & Robotic Systems*, 95(1), 61-75, 2019.
- [14] X. Yang, H., Wu, B., Chen, S., Kang, & S. Cheng. "Dynamic modeling and decoupled control of a flexible Stewart platform for vibration isolation". *Journal of Sound and Vibration*, 439, 398-412, 2019.
- [15] Slotine, E. Jean-Jacques, and Li. Weiping *Applied nonlinear control.* Vol. 199. No. 1. Englewood Cliffs, NJ: prentice-Hall, 1991.